Pergamon

Int. J. Solids Structures Vol. 34, Nos 31–32, pp. 4147–4171, 1997

0020–7683/97 $17.00 + .00

PII: S0020–7683(97)00005–X

CREEP OF METAL-MATRIX COMPOSITES WITH ELASTIC FIBERS—PART I: CONTINUOUS ALIGNED FIBERS

CAO CHENG and N. ARAVAS
Department of Mechanical Engineering and Applied Mechanics, University of Pennsylvania, Philadelphia, PA 19104, U.S.A.

(*Received* 19 *June* 1996; *in revised form* 28 *November* 1996)

Abstract—Three-dimensional constitutive equations are developed for the time-dependent (transient) creep behavior of metal-matrix composites reinforced by continuous elastic fibers. The composite model is developed in two steps: (i) one in which shear loads relative to the fibers are applied and the response is matrix-dominated, and (ii) another in which the composite is subjected to axisymmetric loads relative to the fibers and the response is fiber-dominated. The predictions of the model are compared with the solutions of a number of 'unit cell' problems; periodic boundary conditions, consistent with the requirements of homogenization theory, are imposed on the unit cell, and the solutions are obtained by using the finite element method. A method for the numerical integration of the developed constitutive equations is presented and the material model is implemented in a general-purpose finite element program. © 1997 Elsevier Science Ltd.

1. INTRODUCTION

Metal-matrix composites reinforced by continuous fibers have attracted a lot of attention recently, in view of their potential as high-temperature structural materials. Several *one-dimensional* models that can be used to predict the *creep* behavior of fiber-reinforced composites under simple types of loading are already available in the literature; we mention amongst these the work of Mileiko (1970), Kelly and Street (1972), McLean (1985, 1988, 1989), Goto and McLean (1991a, b), and McMeeking (1993a, b). However, little progress has been made in the development of *three-dimensional* constitutive equations for the behavior of metal-matrix composites at high temperatures.

When both the matrix and the fibers are capable of creeping, the composite exhibits steady-state creep. Three-dimensional constitutive equations for such composites have been developed by Johnson (1977), and more recently by Aravas *et al.* (1995).

When the fibers do not creep, transient creep of the composite is observed (Weber *et al.*, 1993). When such a composite system is subjected to uniaxial tension in the fiber direction, the creeping matrix relaxes, and load is transferred continuously from the matrix to the fibers. Therefore, when the applied macroscopic stress is constant, the axial strain rate decreases with time; eventually, when the matrix stress is completely relaxed, all of the applied load is carried by the fibers and the strain approaches a constant value limited by the elastic deformation of the fibers. McLean (1985, 1988, 1989) developed a model for the response of such composites under uniaxial tension.

In this paper, we develop *three-dimensional* constitutive equations for the *time-dependent* (transient) creep of metal-matrix composites reinforced by continuous elastic fibers. The macroscopic response of the composite is assumed to be transversely isotropic, with the axis of transverse isotropy defined by the direction of the fibers. The composite model is developed in two steps: (i) one in which shear loads relative to the fibers are applied and the response is matrix dominated, and (ii) another in which the composite is subjected to axisymmetric loads relative to the fibers and the response is fiber dominated. The predictions of the model are compared with the solutions of a number of 'unit cell' problems; periodic boundary conditions, consistent with the requirements of homogenization theory, are imposed on the unit cell problems, and the solutions are obtained by using the finite element

method. A method for the numerical integration of the developed constitutive equations is presented. The 'linearization moduli' associated with the integration algorithm are computed, and the proposed new constitutive model is implemented in a general-purpose finite element program.

The effects of fiber failure on behavior of the composite are discussed in detail in Part II of this paper, where a constitutive model that accounts for 'material damage' is developed.

Standard notation is used throughout. Boldface symbols denote tensors the order of which is indicated by the context. All tensor components are written with respect to a fixed Cartesian coordinate system, and the summation convention is used for repeated indices, unless otherwise indicated. A superposed dot indicates the material time derivative, and a superscript T the transpose of a matrix. Let $\mathbf{a}$ and $\mathbf{b}$ be vectors, $\mathbf{A}$ and $\mathbf{B}$ second-order tensors, and $\mathbf{C}$ and $\mathbf{D}$ fourth-order tensors; the following products are used in the text: $(\mathbf{ab})_{ij} = a_i b_j$, $(\mathbf{A}\cdot\mathbf{a})_i = A_{ij}a_j$, $(\mathbf{a}\cdot\mathbf{A})_i = a_j A_{ji}$, $(\mathbf{A}\cdot\mathbf{B})_{ij} = A_{ik}B_{kj}$, $\mathbf{A}:\mathbf{B} = A_{ij}B_{ij}$, $(\partial\mathbf{A}/\partial\mathbf{B})_{ijkl} = \partial A_{ij}/\partial B_{kl}$, $(\mathbf{AB})_{ijkl} = A_{ij}B_{kl}$, $(\mathbf{C}:\mathbf{A})_{ij} = C_{ijkl}A_{kl}$, and $(\mathbf{C}:\mathbf{D})_{ijkl} = C_{ijmn}D_{mnkl}$.

2. DESCRIPTION OF THE MATERIAL SYSTEM

We consider a metal-matrix composite reinforced by continuous aligned fibers. The matrix is considered to exhibit power-law steady-state creep, plus elastic response, such that the tensile strain rate is

$$\dot{\varepsilon} = \frac{\dot{\sigma}}{E_m} + B\sigma^n, \tag{1}$$

where ε and σ are the uniaxial strain and stress, respectively, E_m is the Young's modulus, and (B, n) are the creep constants of the matrix. The fibers behave elastically and the uniaxial stress–strain relationship is

$$\varepsilon = \frac{\sigma}{E_f}, \tag{2}$$

where E_f is the Young's modulus of the fibers. The corresponding three-dimensional version of the above equation is

$$\dot{\boldsymbol{\varepsilon}} = \mathbf{C}_m^{-1} : \dot{\boldsymbol{\sigma}} + \tfrac{3}{2} B\sigma_e^{n-1}\boldsymbol{\sigma}' \quad \text{for the matrix,} \tag{3}$$

and

$$\boldsymbol{\varepsilon} = \mathbf{C}_f^{-1} : \boldsymbol{\sigma} \quad \text{for the fibers,} \tag{4}$$

where $\boldsymbol{\varepsilon}$ and $\boldsymbol{\sigma}$ are the strain and stress tensors, $\mathbf{C}_m$ and $\mathbf{C}_f$ are the fourth-order tensors of the elastic moduli for the matrix and the fibers, respectively, a prime denotes the deviatoric part of a tensor, and $\sigma_e = (1.5\boldsymbol{\sigma}' : \boldsymbol{\sigma}')^{1/2}$ is the von Mises equivalent stress.

It is a well known result that, when the *macroscopic* deformation of the composite is uniform with $\boldsymbol{\varepsilon}$ and $\boldsymbol{\sigma}$ being the corresponding uniform macroscopic fields, then the *average* stresses and strains in the matrix and the fibers are such that

$$\boldsymbol{\sigma} = f\hat{\boldsymbol{\sigma}}_f + (1-f)\hat{\boldsymbol{\sigma}}_m \quad \text{and} \quad \boldsymbol{\varepsilon} = f\hat{\boldsymbol{\varepsilon}}_f + (1-f)\hat{\boldsymbol{\varepsilon}}_m, \tag{5}$$

where the subscripts m and f refer to the matrix and the fibers, respectively, a caret indicates volume average over the phase, and f is the volume fraction of the fibers.

In the following, we let the x_3 coordinate axis coincide with the direction of the fibers, so that the x_1 and x_2 axes are on the transverse plane. An arbitrary macroscopic stress $\boldsymbol{\sigma}$

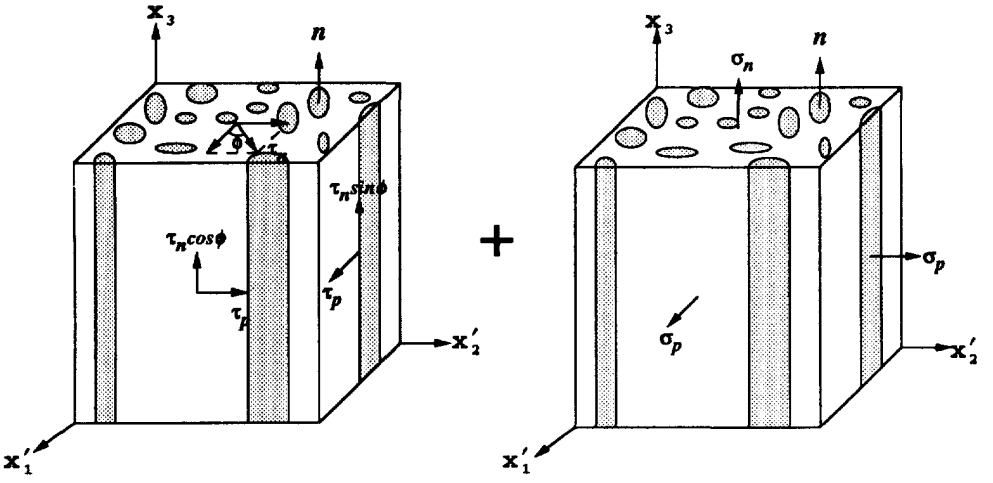

Fig. 1. Representation of an arbitrary stress state.

can be written as

$$\begin{bmatrix} \sigma_{11} & \sigma_{12} & \sigma_{13} \\ \sigma_{12} & \sigma_{22} & \sigma_{23} \\ \sigma_{13} & \sigma_{23} & \sigma_{33} \end{bmatrix} = \begin{bmatrix} \frac{1}{2}(\sigma_{11}-\sigma_{22}) & \sigma_{12} & \sigma_{13} \\ \sigma_{12} & \frac{1}{2}(\sigma_{22}-\sigma_{11}) & \sigma_{23} \\ \sigma_{13} & \sigma_{23} & 0 \end{bmatrix} + \begin{bmatrix} \frac{1}{2}(\sigma_{11}+\sigma_{22}) & 0 & 0 \\ 0 & \frac{1}{2}(\sigma_{11}+\sigma_{22}) & 0 \\ 0 & 0 & \sigma_{33} \end{bmatrix}. \tag{6}$$

The first term on the right hand side of the above equation corresponds to shear loading relative to the fibers, and the last term is the superposition of lateral pressure and uniaxial loading. Therefore, it is always possible to choose the orientation of the x_1 and x_2 axes (say x'_1 and x'_2) so that an arbitrary stress σ can be represented by the superposition of the two states shown in Fig. 1. In terms of the components of the arbitrary stress state of eqn (6), the quantities σ_n, σ_p, τ_n and τ_p shown in Figs 1a and 1b are given by

$$\sigma_n = \sigma_{33}, \quad \sigma_p = \tfrac{1}{2}(\sigma_{11}+\sigma_{22}), \quad \tau_n^2 = \sigma_{13}^2+\sigma_{23}^2, \quad \tau_p^2 = \tfrac{1}{4}(\sigma_{11}-\sigma_{22})^2+\sigma_{12}^2, \tag{7}$$

and are independent of the orientation of the x_1- and x_2-axes.

The behavior of the composite is expected to be substantially different under shear (Fig. 1a) and axisymmetric (Fig. 1b) loading. In particular, the response to the shear loads shown in Fig. 1a will be 'matrix dominated', and the composite is expected to experience 'steady-state' creep, i.e., the creep strain rate is constant under constant applied shear loads; on the other hand, when constant axisymmetric loads are applied, the corresponding creep strain rate will be time-dependent due to matrix relaxation and load transfer from the matrix to the fibers (Weber *et al.* 1993). In the following two Sections 3 and 4, we analyze the behavior of the composite under the two types of loading shown in Fig. 1, and the results are then combined in the constitutive model presented in Section 5.

3. THE MATRIX DOMINATED BEHAVIOR FOR SHEAR LOADING

The creep response of the composite under the shear loading shown in Fig. 1a is dominated by the matrix behavior. The elasticity of the matrix and the fibers are not expected to have a significant influence on the steady-state creep characteristics of the composite under shear. Therefore, for the rest of Section 3, we assume that the fibers are rigid and that the matrix deforms by creep only, i.e., $\mathbf{C}_m^{-1} = \mathbf{C}_f^{-1} = 0$ and $\varepsilon_f = 0$. Referring to Fig. 1a, we assume that the only non-zero stress components are $\sigma_{31'} = \sigma_{1'3} = \tau_n \cos\phi$, $\sigma_{32'} = \sigma_{2'3} = \tau_n \sin\phi$, and $\sigma_{1'2'} = \sigma_{2'1'} = \tau_p$, where the angle ϕ is as shown in Fig. 1a.

In the following, we discuss first a model developed by deBotton and Ponte Castañeda (dB-PC) (1993) for fiber-reinforced nonlinear composites, and then develop a simple model

based on statically admissible stress field and a set of 'unit cell' calculations with periodic boundary conditions.

3.1. *The model of deBotton and Ponte Castañeda*

deBotton and Ponte Castañeda (1993) have recently presented a constitutive model for nonlinear composite materials reinforced by continuous aligned fibers. The derivation of the model is based on a variational principle that enables the expression of the effective energy functions of nonlinear composites in terms of optimization problems. For the case of rigid fibers and a power-law creeping matrix and with respect to the coordinate axes (x_1', x_2', x_3) shown in Fig. 1, their model can be written as

$$[\dot{\boldsymbol{\varepsilon}}] = \tfrac{3}{2}B(1-f)(1+f)^{-(n+1)/2}\sigma_s^{n-1}\begin{bmatrix} 0 & \tau_p & \tau_n\cos\phi \\ \tau_p & 0 & \tau_n\sin\phi \\ \tau_n\cos\phi & \tau_n\sin\phi & 0 \end{bmatrix}, \tag{8}$$

where $\sigma_s^2 = 3(\tau_n^2+\tau_p^2)$. For an arbitrary orientation of the x_1 and x_2 coordinate axes on the transverse plane, the above equations become

$$[\dot{\boldsymbol{\varepsilon}}] = \tfrac{3}{2}B(1-f)(1+f)^{-(n+1)/2}\sigma_s^{n-1}\begin{bmatrix} (\sigma_{11}-\sigma_{22})/2 & \sigma_{12} & \sigma_{13} \\ \sigma_{12} & (\sigma_{22}-\sigma_{11})/2 & \sigma_{23} \\ \sigma_{13} & \sigma_{23} & 0 \end{bmatrix}, \tag{9}$$

where now $\tau_n^2 = \sigma_{13}^2+\sigma_{23}^2$ and $\tau_p^2 = \sigma_{12}^2+(\sigma_{11}-\sigma_{22})^2/4$, so that

$$\sigma_s^2 = \tfrac{3}{4}(\sigma_{11}-\sigma_{22})^2+3(\sigma_{12}^2+\sigma_{13}^2+\sigma_{23}^2). \tag{10}$$

According to this model, constant applied stresses cause constant strain rates (steady-state creep). Also, the predicted response of the composite is identical under longitudinal (σ_{31} or σ_{32}) or transverse (σ_{12}) shear.

An alternative Reuss-type of model is presented in the following Section 3.2 and comparisons with unit cell calculations are presented in Section 3.3.

3.2. *A simple Reuss model*

We assume that the stress tensor in the matrix $\boldsymbol{\sigma}_m$ is *uniform* and equal to the macroscopic stress, i.e., $\boldsymbol{\sigma}_m = \boldsymbol{\sigma}$. The corresponding uniform strain rate in the matrix is

$$\dot{\boldsymbol{\varepsilon}}_m = \dot{\hat{\boldsymbol{\varepsilon}}}_m = \tfrac{3}{2}B\sigma_e^{n-1}\boldsymbol{\sigma}'. \tag{11}$$

In view of eqn (5b), the macroscopic strain rate $\dot{\boldsymbol{\varepsilon}}$ is now

$$\dot{\boldsymbol{\varepsilon}} = (1-f)\dot{\hat{\boldsymbol{\varepsilon}}}_m = \tfrac{3}{2}B(1-f)\sigma_e^{n-1}\boldsymbol{\sigma}', \tag{12}$$

or

$$[\dot{\boldsymbol{\varepsilon}}] = \tfrac{3}{2}B(1-f)\sigma_s^{n-1}\begin{bmatrix} 0 & \tau_p & \tau_n\cos\phi \\ \tau_p & 0 & \tau_n\sin\phi \\ \tau_n\cos\phi & \tau_n\sin\phi & 0 \end{bmatrix}, \quad \sigma_s^2 = \sigma_e^2 = 3(\tau_n^2+\tau_p^2), \tag{13}$$

with respect to the coordinate axes (x_1', x_2', x_3) shown in Fig. 1. When the orientation of the x_1 and x_2 coordinate axes on the transverse plane is arbitrary, the above equation for the macroscopic strain rate can be written as

$$[\dot{\varepsilon}] = \tfrac{3}{2}B(1-f)\sigma_s^{n-1}\begin{bmatrix}(\sigma_{11}-\sigma_{22})/2 & \sigma_{12} & \sigma_{13}\\ \sigma_{12} & (\sigma_{22}-\sigma_{11})/2 & \sigma_{23}\\ \sigma_{23} & \sigma_{23} & 0\end{bmatrix}, \tag{14}$$

where

$$\sigma_s^2 = \sigma_e^2 = \tfrac{3}{4}(\sigma_{11}-\sigma_{22})^2 + 3(\sigma_{12}^2+\sigma_{13}^2+\sigma_{23}^2). \tag{15}$$

It is interesting to note that the form of eqn (14) is identical to that of (9), the only difference being the multiplicative constant $(1+f)^{-(n+1)/2} < 1$ in (9).

3.3. *Unit cell solutions*

The predictions of the analytical models discussed in the previous subsections are compared with the results of periodic homogenization theory (Sanchez-Palencia, 1980; Bakhvalov and Panasenko, 1989). A number of 'unit cell' problems with periodic boundary conditions, consistent with the requirements of homogenization theory, are solved by using the finite element method. The distribution of the fibers is assumed to be periodic, with the fibers arranged in a hexagonal array. A detailed description of the formulation of the unit cell problems can be found in Aravas *et al.* (1993) and Cheng (1996) and will not be repeated here.

The macroscopic applied loads are combinations of transverse and longitudinal shear. Figure 2 shows the assumed hexagonal arrangement of the fibers in the matrix, and Fig. 3 shows the finite element mesh used in the two-dimensional calculations. The dark and white regions in Fig. 3 represent the fibers and the matrix respectively. A similar mesh is used in the three-dimensional calculations that involve longitudinal shear (Aravas *et al.*, 1993). Calculations are carried out for several values of the matrix creep exponent n and for different values of the fiber volume fraction f. The numerical solution is practically independent of the values of the elastic constants of the fibers and the matrix. It is found that the results of the unit cell calculations agree very well with a constitutive equation of the

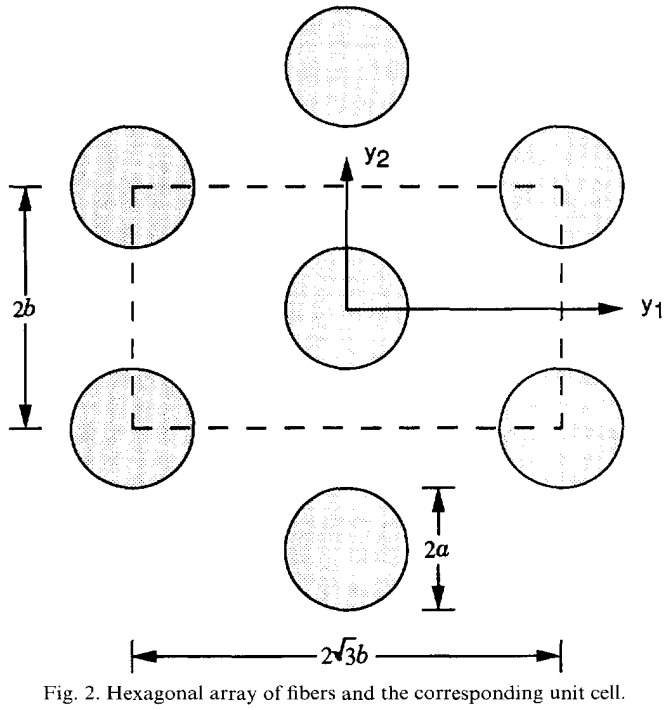

Fig. 2. Hexagonal array of fibers and the corresponding unit cell.

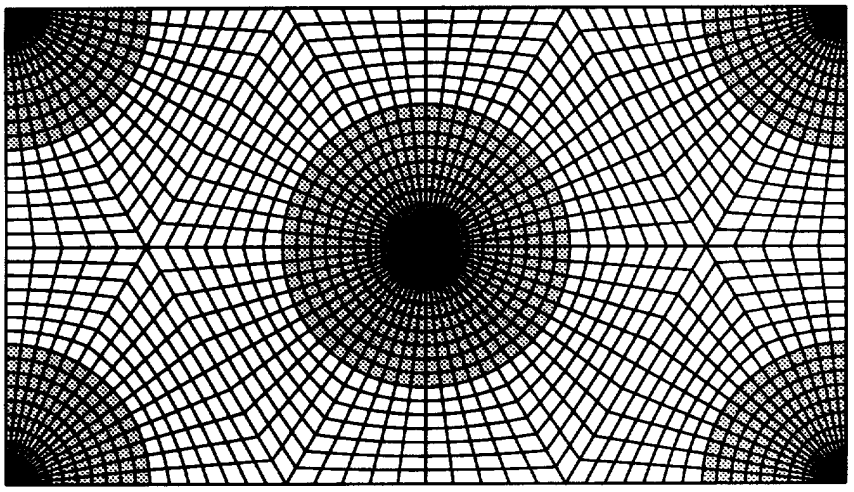

Fig. 3. Finite element mesh used in the unit cell calculations.

form

$$[\dot{\varepsilon}] = \tfrac{3}{2}B(1-f)\chi^n\sigma_s^{n-1}\begin{bmatrix}(\sigma_{11}-\sigma_{22})/2 & \sigma_{12} & \sigma_{13}\\ \sigma_{12} & (\sigma_{22}-\sigma_{11})/2 & \sigma_{23}\\ \sigma_{13} & \sigma_{23} & 0\end{bmatrix}, \tag{16}$$

where $\chi = \chi(n,f)$, and the orientation of the x_1 and x_2 axes on the transverse plane is arbitrary. Note that $\chi = (1+f)^{-(n+1)/(2n)}$ in the dB-PC model, and $\chi = 1$ in the Reuss model of Section 3.2.

It is noteworthy that the unit cell calculations predict that the response is identical under longitudinal and transverse shear as well. The results of the finite element solutions indicate that, for values of n and f in the range $1 \leqslant n \leqslant 10$ and $0 \leqslant f \leqslant 0.70$, the quantity χ^{-1} can be approximated by an equation of the form:

$$\chi^{-1} = 1 + a(n)f + b(n)f^2 + c(n)f^6, \tag{17}$$

where $a(n)$ is given by

$$a(n) = \frac{1}{4G(n)}\left(\frac{n+1}{n}\right)^2 - \frac{n+1}{2n^2}, \quad G(n) = \frac{1}{2}\left(\frac{n+1}{\sqrt{n}+1}\right), \tag{18}$$

and

$$b(n) = \frac{0.467}{n} - 0.248 - 0.009n, \quad c(n) = \frac{15.199}{n} + 1.132 + 0.248n. \tag{19}$$

For composite materials with a *statistically isotropic* (as opposed to period) microstructure, Ponte Castañeda (1996) obtained the following exact result for the dilute limit (small f):

$$\chi^{-1} = 1 + a(n)f. \tag{20}$$

For small values of f, the interaction between neighboring fibers is very weak, and eqn (20) is also valid for composites with a *periodic* microstructure. Note that the expression for χ^{-1} in eqn (17) is consistent with the exact result (20) in the limit of small f.

For the case of transverse macroscopic shear loading ($\sigma_{12} = \tau$), the above model

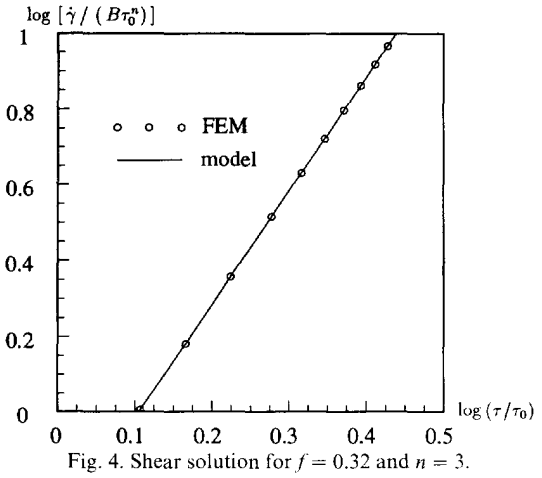

Fig. 4. Shear solution for $f = 0.32$ and $n = 3$.

predicts

$$\frac{\dot{\gamma}}{B\tau_0^n} = 3^{(n+1)/2}(1-f)\chi^n\left(\frac{\tau}{\tau_0}\right)^n, \tag{21}$$

where $\gamma = 2\varepsilon_{12}$, and τ_0 is an arbitrary reference stress. Figure 4 shows the results of the unit cell calculations together with those of eqns (17)–(21) for $f = 0.32$ and $n = 3$. The predictions of the analytical model agree well with the results of the finite element solutions.

4. THE FIBER DOMINATED BEHAVIOR FOR AXISYMMETRIC LOADING

In the case of the axisymmetric loading shown in Fig. 1b, the elasticity of the fibers is of major importance. In the following, we discuss first a simple model developed by McLean (1985, 1988) for uniaxial tension in the direction of the fibers, and then develop a three-dimensional version of it for the case of the axisymmetric loading shown in Fig. 1b.

4.1. *McLean's model for uniaxial tension in the direction of the fibers*

The macroscopic applied load is tensile in the direction of the fibers, i.e., $\sigma_{33} = \sigma$. Let $\varepsilon_{33} = \varepsilon$ be the corresponding macroscopic axial strain component.

McLean assumes that the stresses take *constant* values in the fibers and the matrix and that the only non-zero components are $\sigma_{f33} = \sigma_f$ and $\sigma_{m33} = \sigma_m$. He also assumes that the corresponding uniform axial strain in the fibers and the matrix equals the macroscopic axial strain ε. With these assumptions, eqn (5a) implies that

$$\sigma = f\sigma_f + (1-f)\sigma_m, \tag{22}$$

and the axial strain rate can be written as

$$\dot{\varepsilon} = \frac{\dot{\sigma}_f}{E_f} = \frac{\dot{\sigma}_m}{E_m} + B\sigma_m^n. \tag{23}$$

Using the last two equations we can readily show that McLean model can be written in the following form:

$$\dot{\varepsilon} = \frac{\dot{\sigma}}{E} + B'(\sigma-\alpha)^n \quad \text{and} \quad \frac{\dot{\alpha}}{fE_f} = \frac{\dot{\sigma}}{E} + B'(\sigma-\alpha)^n, \tag{24}$$

where the 'back stress' $\alpha = f\sigma_f$ is the part of the total axial stress carried by the fibers (see eqn (22)), $E = fE_f + (1-f)E_m$, and $B' = BE_m/[(1-f)^{n-1}E]$. The initial values of the strain (ε_0) and the back stress (α_0) at the start of the loading history (time $t = 0^-$) are

$$\varepsilon_0 = \sigma(0^+)/E \quad \text{and} \quad \alpha_0 = fE_f\varepsilon_0. \tag{25}$$

The first term on the right hand side of (24a) defines the elastic strain rate in the composite ($\dot{\varepsilon}^e$), and the second term defines the macroscopic creep strain rate $\dot{\varepsilon}^{cr}$. Equation (24a) for the composite has a form similar to that of the matrix (23b) or (1), where now E_m is replaced by E in the elastic part, and B and σ by B' and $\sigma-\alpha$, respectively, in the creep part of $\dot{\varepsilon}$. The back stress α is a measure of the stress carried by the fibers and accounts for the strengthening effects of the fibers; i.e., whereas the creep strain rate is proportional to σ^n in the absence of fibers, $\dot{\varepsilon}^{cr}$ is proportional to $(\sigma-\alpha)^n$ when $f \neq 0$.

For the case of a 'creep test' in which a constant stress σ is applied in the direction of the fibers, eqns (24) make it clear that the strain rate varies with time due to the evolution of the back stress α (transient or non-steady-state creep). In this case, eqns (24) can be integrated to give

$$\varepsilon(t) = \varepsilon_c\left\{1-\left(1-\frac{\varepsilon_0}{\varepsilon_c}\right)\left[1+(n-1)\left(1-\frac{\varepsilon_0}{\varepsilon_c}\right)^{n-1}\frac{B'\sigma^n t}{\varepsilon_c}\right]^{-1/(n-1)}\right\} \quad \text{for } n>1, \tag{26}$$

$$\varepsilon(t) = \varepsilon_c\left[1-\left(1-\frac{\varepsilon_0}{\varepsilon_c}\right)\exp\left(-\frac{B'\sigma^n t}{\varepsilon_c}\right)\right] \quad \text{for } n=1, \tag{27}$$

and

$$\alpha(t) = fE_f\varepsilon(t), \tag{28}$$

where $\varepsilon_0 = \sigma/E$, and $\varepsilon_c = \sigma/(fE_f)$. In the uniaxial creep test, as the matrix creeps, the corresponding stress σ_m relaxes, load is transferred from the matrix to the fibers and, as a consequence, the back stress α increases with time. The long time response of the system as $t \to \infty$ is such that

$$\dot{\varepsilon} \to 0, \quad \varepsilon \to \varepsilon_c, \quad \sigma_m \to 0, \quad \text{and} \quad \alpha = f\sigma_f \to \sigma, \tag{29}$$

i.e., eventually the strain approaches the limiting value ε_c, the matrix is completely unloaded and the whole load is carried by the fibers. Figure 5 shows the variation of the normalized

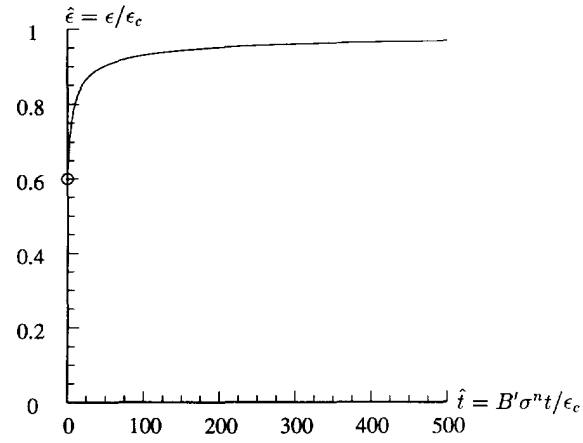

Fig. 5. Uniaxial tension solution for $\varepsilon_0/\varepsilon_c = 0.6$ and $n = 3$.

strain $\hat{\varepsilon}$ with normalized time $\hat{t}$ for values of $n = 3$ and $\varepsilon_0/\varepsilon_c = 0.6$, where

$$\hat{\varepsilon} = \frac{\varepsilon}{\varepsilon_c} = \frac{\alpha}{\sigma} \quad \text{and} \quad \hat{t} = \frac{B'\sigma^n t}{\varepsilon_c}. \tag{30}$$

4.2. *A three-dimensional version of the McLean model*

We consider next the case in which the applied macroscopic load is axisymmetric of the form shown in Fig. 1b, i.e., $\sigma_{1'1'} = \sigma_{2'2'} = \sigma_p$ and $\sigma_{33} = \sigma_n$. Note that this macroscopic stress state maintains its form for an arbitrary orientation of the x_1- and x_2-axes on the transverse plane, i.e., it is always true that $\sigma_{11} = \sigma_{22} = \sigma_p$.

Assumptions similar to those of McLean are used for this type of loading as well; i.e., it is assumed that

1. the stresses take constant values in the fibers and the matrix, i.e,

$$[\boldsymbol{\sigma}_f] = \begin{bmatrix} \sigma_p & 0 & 0 \\ 0 & \sigma_p & 0 \\ 0 & 0 & \sigma_f \end{bmatrix} \quad \text{and} \quad [\boldsymbol{\sigma}_m] = \begin{bmatrix} \sigma_p & 0 & 0 \\ 0 & \sigma_p & 0 \\ 0 & 0 & \sigma_m \end{bmatrix}, \tag{31}$$

   where the transverse normal stresses are taken to be equal to the macroscopic load σ_p, and
2. the corresponding axial strain in the fibers and the matrix is equal to the axial macroscopic strain $\varepsilon_{33} = \varepsilon$, i.e.,

$$\varepsilon_{f33} = \varepsilon_{m33} = \varepsilon. \tag{32}$$

In view of eqn (5a), the axial components σ_f and σ_m are such that

$$\sigma_n = f\sigma_f + (1-f)\sigma_m. \tag{33}$$

Recalling eqn (5b) we write $\dot{\boldsymbol{\varepsilon}} = f\dot{\boldsymbol{\varepsilon}}_f + (1-f)\dot{\boldsymbol{\varepsilon}}_m$, and using the constitutive eqns (3) and (4) for the matrix and the fibers respectively we find

$$\begin{Bmatrix} \dot{\varepsilon}_{11} \\ \dot{\varepsilon}_{22} \\ \dot{\varepsilon}_{33} \end{Bmatrix} = \frac{f}{E_f}\begin{bmatrix} 1 & -\nu_f & -\nu_f \\ -\nu_f & 1 & -\nu_f \\ -\nu_f & -\nu_f & 1 \end{bmatrix}\begin{Bmatrix} \dot{\sigma}_p \\ \dot{\sigma}_p \\ \dot{\sigma}_f \end{Bmatrix} + \frac{1-f}{E_m}\begin{bmatrix} 1 & -\nu_m & -\nu_m \\ -\nu_m & 1 & -\nu_m \\ -\nu_m & -\nu_m & 1 \end{bmatrix}\begin{Bmatrix} \dot{\sigma}_p \\ \dot{\sigma}_p \\ \dot{\sigma}_m \end{Bmatrix}$$
$$+ (1-f)\frac{B}{2}|\sigma_m - \sigma_p|^{n-1}(\sigma_m - \sigma_p)\begin{Bmatrix} -1 \\ -1 \\ 2 \end{Bmatrix}. \tag{34}$$

Our goal is to eliminate the 'local' stresses σ_m and σ_f from the above equation and arrive at an expression for $\dot{\boldsymbol{\varepsilon}}$ in terms of the macroscopic stresses σ_n, σ_p and a back stress α. This is achieved as follows.

As before, we introduce the back stress $\alpha = f\sigma_f$, and using (33) we write

$$\sigma_m = \frac{\sigma_n - \alpha}{1-f} \quad \text{and} \quad \sigma_f = \frac{\alpha}{f}. \tag{35}$$

Next, we use the strain continuity equation $\dot{\varepsilon}_{f33} = \dot{\varepsilon}_{m33}$ together with the constitutive equations for the fibers and the matrix and eqns (35) to determine $\dot{\alpha}$ in terms of $\dot{\sigma}_n$, $\dot{\sigma}_p$, σ_n, σ_p, and α:

$$\frac{\dot{\alpha}}{fE_f}=\frac{\dot{\sigma}_n}{E_L}+2(1-f)\left(\frac{E_m}{E_f}\nu_f-\nu_m\right)\frac{\dot{\sigma}_p}{E_L}+B'(1-f)^n\left|\frac{\sigma_n-\alpha}{1-f}-\sigma_p\right|^{n-1}\left(\frac{\sigma_n-\alpha}{1-f}-\sigma_p\right), \tag{36}$$

where

$$E_L=E=fE_f+(1-f)E_m \quad \text{and} \quad B'=\frac{BE_m}{(1-f)^{n-1}E_L}. \tag{37}$$

Finally, substituting eqns (35) into (34) and using the expression for $\dot{\alpha}$, we obtain the following equation for the macroscopic strain rates:

$$\begin{Bmatrix}\dot{\varepsilon}_{11}\\ \dot{\varepsilon}_{22}\\ \dot{\varepsilon}_{33}\end{Bmatrix}=\begin{bmatrix}1/E_T & -\nu_T/E_T & -\nu_T/E_L\\ -\nu_T/E_T & 1/E_T & -\nu_L/E_L\\ -\nu_L/E_L & -\nu_L/E_L & 1/E_L\end{bmatrix}\begin{Bmatrix}\dot{\sigma}_p\\ \dot{\sigma}_p\\ \dot{\sigma}_n\end{Bmatrix}+B'(1-f)^n\left|\frac{\sigma_n-\alpha}{1-f}-\sigma_p\right|^{n-1}\left(\frac{\sigma_n-\alpha}{1-f}-\sigma_p\right)\begin{Bmatrix}K'\\ K'\\ 1\end{Bmatrix}, \tag{38}$$

where

$$\frac{1}{E_T}=\frac{1-f}{E_m}+\frac{f}{E_f}+2f(1-f)\frac{E_f}{E_L}\left(\frac{E_m}{E_f}\nu_f-\nu_m\right)\left(\frac{\nu_m}{E_m}-\frac{\nu_f}{E_f}\right), \tag{39}$$

$$\frac{\nu_T}{E_T}=(1-f)\frac{\nu_m}{E_m}+f\frac{\nu_f}{E_f}, \quad \nu_L=f\nu_f+(1-f)\nu_m, \tag{40}$$

and

$$K'=-\frac{1}{2}+f\left[\frac{E_f}{E_m}\left(\nu_m-\frac{1}{2}\right)-\left(\nu_f-\frac{1}{2}\right)\right]. \tag{41}$$

The initial value of the back stress α_0 is

$$\alpha_0=\frac{fE_f}{E_L}\left[\sigma_n(0^+)-2(1-f)E_m\left(\frac{\nu_m}{E_m}-\frac{\nu_f}{E_f}\right)\sigma_p(0^+)\right]. \tag{42}$$

The first term on the right hand side of (38) defines the elastic part $\dot{\boldsymbol{\varepsilon}}^e$ of the total strain rate and the second term defines the macroscopic creep strain rate $\dot{\boldsymbol{\varepsilon}}^{cr}$. In order to make connection with eqn (16) for $\dot{\boldsymbol{\varepsilon}}^{cr}$ in the case of shear loading, we note that the second term on the right hand side of (38) can be also written as

$$[\dot{\boldsymbol{\varepsilon}}^{cr}]=\frac{3}{2}B(1-f)|S|^{n-1}\begin{bmatrix}KS & 0 & 0\\ 0 & KS & 0\\ 0 & 0 & LS\end{bmatrix}, \quad \text{where } S=\frac{\sigma_n-\alpha}{1-f}-\sigma_p, \tag{43}$$

and

$$K=\frac{2}{3}\frac{E_m}{E_L}\left\{-\frac{1}{2}+f\left[\frac{E_f}{E_m}\left(\nu_m-\frac{1}{2}\right)-\left(\nu_f-\frac{1}{2}\right)\right]\right\}, \quad L=\frac{2}{3}\frac{E_m}{E_L}. \tag{44}$$

4.3. *Unit cell solutions*

The predictions of the model developed in the previous section are now compared with unit-cell finite element calculations. Periodic boundary conditions, similar to those described

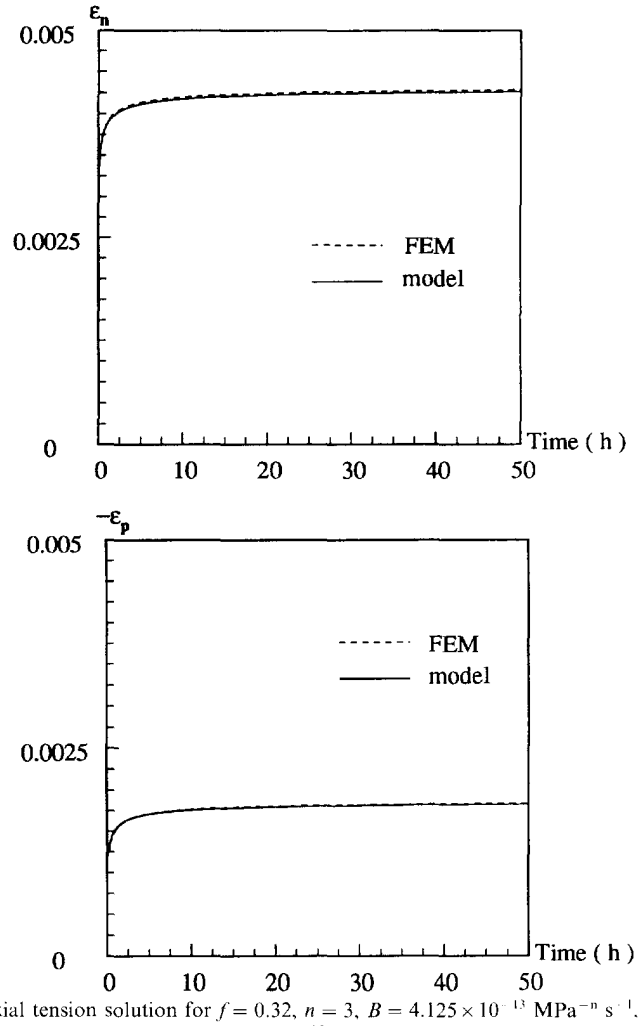

Fig. 6. Uniaxial tension solution for $f = 0.32$, $n = 3$, $B = 4.125 \times 10^{-13}$ MPa^{-n} s^{-1}, and $\sigma_n = 500$ MPa.

in Section 3.3, are imposed. The material properties used in the calculations are $E_f = 360$ GPa, $\nu_f = 0.3$, $E_m = 65$ GPa, $\nu_m = 0.3$, $n = 3$, and $B = 4.125 \times 10^{-13}$ MPa^{-n}s^{-1}. The volume fraction of the fibers is $f = 0.32$.

Figure 6 shows the results of the finite element calculations together with the predictions of the model (38)–(42), when a constant axial macroscopic load $\sigma_n = 500$ MPa is applied. The corresponding results for a constant axisymmetric transverse macroscopic load $\sigma_p = 100$ MPa are shown in Fig. 7. The results of the unit cell calculations agree well with the predictions of the analytical model.

5. A PROPOSED NEW MODEL

The results derived in Sections 3 and 4 for shear and axisymmetric loadings, respectively, are now combined and constitutive equations for general types of loading are developed. Clearly, in view of the non-linearity of the problem, the equations developed for shear and axisymmetric loadings can not be superposed. Instead, our results are combined in such a way that the proposed general constitutive equations for $\dot{\boldsymbol{\varepsilon}}^{cr}$ reduce to eqns (16) and (43) when the applied loads are shear or axisymmetric, respectively.

The detailed description of the proposed model is presented in the following two subsections. The macroscopic response of the composite is transversely isotropic, and the unit vector **n** in the direction of the fibers is used to define the axis of rotational symmetry. The

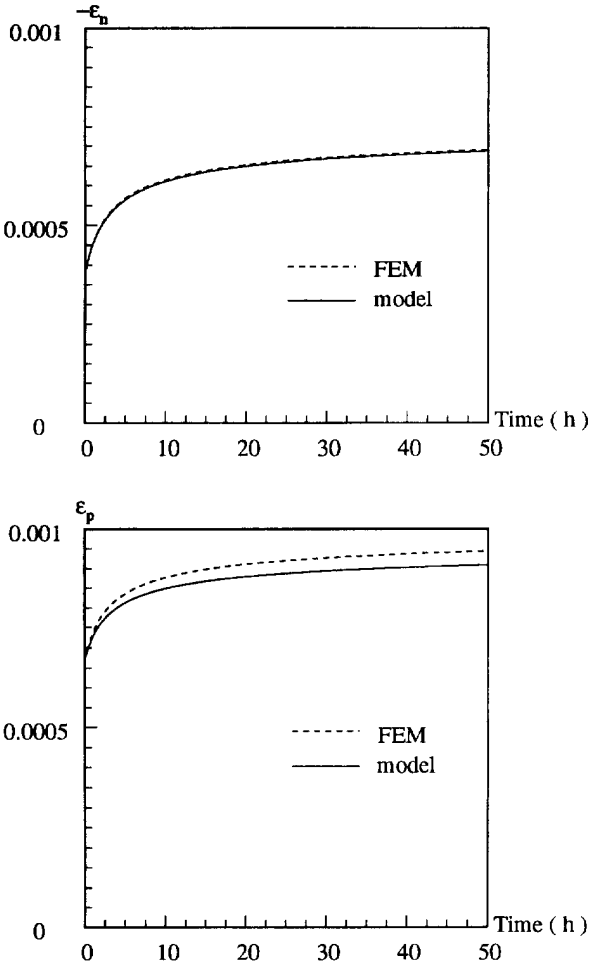

Fig. 7. Biaxial tension solution for $f = 0.32$, $n = 3$, $B = 4.125 \times 10^{-13}$ MPa^{-n} s^{-1}, and $\sigma_n = 100$ MPa.

total macroscopic strain in the composite is written as the sum of the elastic and creep parts:

$$\boldsymbol{\varepsilon} = \boldsymbol{\varepsilon}^e + \boldsymbol{\varepsilon}^{cr}. \tag{45}$$

Constitutive equations for $\boldsymbol{\varepsilon}^e$ and $\dot{\boldsymbol{\varepsilon}}^{cr}$ are presented in the following.

5.1. *Elasticity*

The elastic strain is written in terms of the stress tensor $\boldsymbol{\sigma}$ as

$$\boldsymbol{\varepsilon}^e = \mathbf{C}^{e-1} : \boldsymbol{\sigma}, \tag{46}$$

where $\mathbf{C}^e$ is the fourth-order elasticity tensor for the homogenized transversely isotropic composite. When the fibers are aligned with the x_3 coordinate direction (i.e., $\mathbf{n} = \mathbf{e}_3$), eqn (46) can be written in matrix form as

$$\{\boldsymbol{\varepsilon}^e\} = [\mathbf{C}^e]^{-1}\{\boldsymbol{\sigma}\}, \tag{47}$$

where $\{\boldsymbol{\varepsilon}^e\}^T = \{\varepsilon^e_{11}, \varepsilon^e_{22}, \varepsilon^e_{33}, \gamma^e_{12}, \gamma^e_{13}, \gamma^e_{23}\}$, $\{\boldsymbol{\sigma}\}^T = \{\sigma_{11}, \sigma_{22}, \sigma_{33}, \sigma_{12}, \sigma_{13}, \sigma_{23}\}$,

$$[\mathbf{C}^e]^{-1} = \begin{bmatrix} 1/E_T & -\nu_T/E_T & -\nu_L/E_L & 0 & 0 & 0 \\ -\nu_T/E_T & 1/E_T & -\nu_L/E_L & 0 & 0 & 0 \\ -\nu_L/E_L & -\nu_L/E_L & 1/E_L & 0 & 0 & 0 \\ 0 & 0 & 0 & 1/G_T & 0 & 0 \\ 0 & 0 & 0 & 0 & 1/G_L & 0 \\ 0 & 0 & 0 & 0 & 0 & 1/G_L \end{bmatrix},$$

E_L, E_T, G_L, ν_L and ν_T are the five independent elastic constants of the composite, and

$$G_T = \frac{E_T}{2(1+\nu_T)}. \tag{48}$$

The constants E_L, E_T, ν_L and ν_T are defined by eqns (37a), (39), and (40), and the shear modulus G_L is estimated as (Christensen, 1979, p. 84)

$$G_L = G_m \frac{G_f(1+f)+G_m(1-f)}{G_f(1-f)+G_m(1+f)}, \tag{49}$$

where G_f and G_m are the shear moduli of the fibers and the matrix, respectively.

5.2. *Creep*

The general form of the constitutive equations during creep is

$$\dot{\boldsymbol{\varepsilon}}^{cr} = \mathbf{g}(\boldsymbol{\sigma}-\boldsymbol{\alpha}, s), \quad \dot{\boldsymbol{\alpha}} = \mathbf{h}(\boldsymbol{\sigma}-\boldsymbol{\alpha}, \dot{\boldsymbol{\sigma}}, s), \tag{50}$$

where $\boldsymbol{\alpha}$ is the back stress tensor, $\mathbf{g}$ and $\mathbf{h}$ are tensor-valued isotropic functions, and s is the collection of material parameters, $s = \{E_f, \nu_f, E_m, \nu_m, B, n, f\}$. In the present model, the back stress tensor $\boldsymbol{\alpha}$ is assumed to be in the direction of the fibers, i.e, $\boldsymbol{\alpha} = \alpha\mathbf{nn}$; it should be noted, however, that more complicated forms may be necessary when effects such as the primary (transient) creep of the matrix must be accounted for.

In the following, we combine the results of Sections 3 and 4 and develop constitutive equations for general types of loading. The proposed model is such that eqns (16) and (38) are recovered as special cases, when the applied loads are shear or axisymmetric, respectively. With respect to the coordinate axes shown in Fig. 1 and for an arbitrary orientation of the x_1–x_2 axes on the transverse plane, we write the following equations for the creep strain rate:

$$[\dot{\boldsymbol{\varepsilon}}^{cr}] = \frac{3}{2}B(1-f)\,\Sigma_e^{n-1}\begin{bmatrix} \chi(\sigma_{11}-\sigma_{22})/2+KS & \chi\sigma_{12} & \chi\sigma_{13} \\ \chi\sigma_{12} & \chi(\sigma_{22}-\sigma_{11})/2+KS & \chi\sigma_{23} \\ \chi\sigma_{13} & \chi\sigma_{23} & LS \end{bmatrix}, \tag{51}$$

where $\Sigma_e^2 = S^2+(\chi\sigma_s)^2$. For convenience, we repeat the definition of the quantities entering the above equation: $\sigma_n = \sigma_{33}$, $\sigma_p = (\sigma_{11}+\sigma_{22})/2$,

$$S = \frac{\sigma_n-\alpha}{1-f} - \sigma_p, \quad \sigma_s^2 = \frac{3}{4}(\sigma_{11}-\sigma_{22})^2+3(\sigma_{12}^2+\sigma_{13}^2+\sigma_{23}^2), \tag{52}$$

$$K = \frac{2}{3}\frac{E_m}{E_L}\left\{-\frac{1}{2}+f\left[\frac{E_f}{E_m}\left(\nu_m-\frac{1}{2}\right)-\left(\nu_f-\frac{1}{2}\right)\right]\right\}, \quad L = \frac{2}{3}\frac{E_m}{E_L}, \tag{53}$$

and recall that $\chi(n,f)$ is defined by eqns (17)–(19). The evolution of the back stress is given

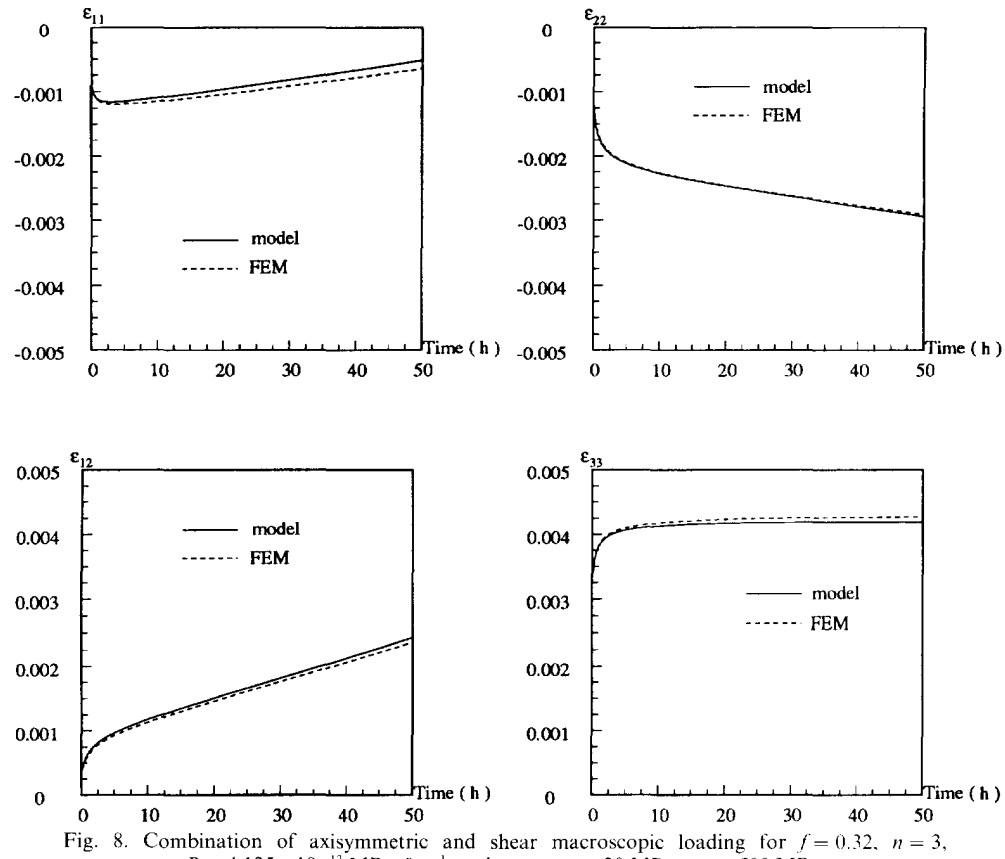

Fig. 8. Combination of axisymmetric and shear macroscopic loading for $f = 0.32$, $n = 3$, $B = 4.125 \times 10^{-13}$ MPa^{-n} s^{-1}, and $\sigma_{11} = \sigma_{12} = 20$ MPa, $\sigma_{33} = 500$ MPa.

by

$$\frac{\dot{\alpha}}{fE_f} = \frac{\dot{\sigma}_n}{E_L} + 2(1-f)\left(\frac{E_m}{E_f}\nu_f - \nu_m\right)\frac{\dot{\sigma}_p}{E_L} + B'(1-f)^n \Sigma_e^{n-1}\left(\frac{\sigma_n - \alpha}{1-f} - \sigma_p\right), \tag{54}$$

where E_L and B' are defined by (37), and the initial value of α_0 of the back stress is given by eqn (42).

5.3. *Unit cell solutions*

The predictions of the proposed new model are compared with the results of finite element calculations, in which a unit cell is subjected to a combination of axisymmetric and shear macroscopic loading. The material constants mentioned in Section 4.3 are used in the present calculations as well. Figure 8 shows the temporal variation of various strain components for the case where constant macroscopic stresses $\sigma_{11} = 20$ MPa, $\sigma_{12} = 20$ MPa, and $\sigma_{33} = 500$ MPa are applied to the unit cell. The results of the numerical calculations agree well with the predictions of the analytical model.

6. FINITE ELEMENT IMPLEMENTATION OF THE CONSTITUTIVE MODEL

In this section, we discuss the implementation of the general form of the proposed constitutive model in a finite element program. In a finite element environment, the solution of the creep problem is developed incrementally and the constitutive equations are integrated numerically at the element Gauss points. In a displacement based finite element formulation the solution is deformation driven. At a material point, the solution $(\boldsymbol{\sigma}_n, \boldsymbol{\varepsilon}_n, \boldsymbol{\alpha}_n)$ at time t_n as well as the strain $\boldsymbol{\varepsilon}_{n+1}$ at time $t_{n+1} = t_n + \Delta t$ are supposed to be known and one has to determine the solution $(\boldsymbol{\sigma}_{n+1}, \boldsymbol{\alpha}_{n+1})$.

6.1. *Numerical integration of the constitutive equations*

We start with the elasticity eqn (46)

$$\boldsymbol{\sigma}_{n+1} = \mathbf{C}^e : \boldsymbol{\varepsilon}^e_{n+1} = \mathbf{C}^e : (\boldsymbol{\varepsilon}^e_n + \Delta\boldsymbol{\varepsilon} - \Delta\boldsymbol{\varepsilon}^{cr}) = \boldsymbol{\sigma}^e - \mathbf{C}^e : \Delta\boldsymbol{\varepsilon}^{cr}, \tag{55}$$

where $\Delta\boldsymbol{\varepsilon} = \boldsymbol{\varepsilon}_{n+1} - \boldsymbol{\varepsilon}_n$ and $\Delta\boldsymbol{\varepsilon}^{cr} = \boldsymbol{\varepsilon}^{cr}_{n+1} - \boldsymbol{\varepsilon}^{cr}_n$ are the total- and creep-strain increments, and $\boldsymbol{\sigma}^e = \boldsymbol{\sigma}_n + \mathbf{C}^e : \Delta\boldsymbol{\varepsilon}$ is the (known) 'elastic predictor'.

The constitutive eqns (51) and (54) for $\dot{\boldsymbol{\varepsilon}}^{cr}$ and $\dot{\boldsymbol{\alpha}}$ are integrated by using the backward Euler method:

$$\Delta\boldsymbol{\varepsilon}^{cr} = \mathbf{g}(\boldsymbol{\sigma}_{n+1} - \boldsymbol{\alpha}_{n+1})\,\Delta t, \tag{56}$$

$$\Delta\boldsymbol{\alpha} = \mathbf{h}(\boldsymbol{\sigma}_{n+1} - \boldsymbol{\alpha}_{n+1}, \Delta\boldsymbol{\sigma}/\Delta t)\,\Delta t, \tag{57}$$

where $\Delta\boldsymbol{\sigma} = \boldsymbol{\sigma}_{n+1} - \boldsymbol{\sigma}_n$.

Summarizing, we write

$$\mathbf{G}(\Delta\boldsymbol{\varepsilon}^{cr}, \Delta\boldsymbol{\alpha}) \equiv \Delta\boldsymbol{\varepsilon}^{cr} - \Delta t\mathbf{g}(\boldsymbol{\sigma}_{n+1} - \boldsymbol{\alpha}_n - \Delta\boldsymbol{\alpha}) = 0, \tag{58}$$

$$\mathbf{H}(\Delta\boldsymbol{\varepsilon}^{cr}, \Delta\boldsymbol{\alpha}) \equiv \Delta\boldsymbol{\alpha} - \Delta t\mathbf{h}\left(\boldsymbol{\sigma}_{n+1} - \boldsymbol{\alpha}_n - \Delta\boldsymbol{\alpha}, \frac{\boldsymbol{\sigma}_{n+1} - \boldsymbol{\sigma}_n}{\Delta t}\right) = 0, \tag{59}$$

where

$$\boldsymbol{\sigma}_{n+1}(\Delta\boldsymbol{\varepsilon}^{cr}) = \boldsymbol{\sigma}^e - \mathbf{C}^e : \Delta\boldsymbol{\varepsilon}^{cr}. \tag{60}$$

We choose $\Delta\boldsymbol{\varepsilon}^{cr}$ and $\Delta\boldsymbol{\alpha}$ as the primary unknowns and treat (58) and (59) as the basic equations in which $\boldsymbol{\sigma}_{n+1}$ is defined by (60). The solution is obtained by using Newton's method. The first estimate for $\Delta\boldsymbol{\varepsilon}^{cr}$ and $\Delta\boldsymbol{\alpha}$ used to start the Newton loop are obtained by using a forward Euler scheme, i.e., $(\Delta\boldsymbol{\varepsilon}^{cr})_{\text{est}} = \mathbf{g}(\boldsymbol{\sigma}_n - \boldsymbol{\alpha}_n)\,\Delta t$ and $(\Delta\boldsymbol{\alpha})_{est} = \mathbf{h}(\boldsymbol{\sigma}_n - \boldsymbol{\alpha}_n, \Delta\boldsymbol{\sigma}_n/\Delta t)\,\Delta t$, where $\Delta\boldsymbol{\sigma}_n = \boldsymbol{\sigma}_n - \boldsymbol{\sigma}_{n-1}$.

Once $\Delta\boldsymbol{\varepsilon}^{cr}$ and $\Delta\boldsymbol{\alpha}$ are found, eqn (60) defines the stress $\boldsymbol{\sigma}_{n+1}$, $\boldsymbol{\alpha}_{n+1} = \boldsymbol{\alpha}_n + \Delta\boldsymbol{\alpha}$, and this completes the integration procedure.

We conclude this section with a brief discussion of the appropriate time increment used in the integration procedure. Let σ_{max} be the maximum of the absolute values of the stress components (i.e., $\sigma_{max} = \max|\sigma_{ij}|_{n+1}$) and define

$$\text{CETOL} = 0.1 \times \frac{\sigma_{max}}{(E_L + E_T)/2}, \tag{61}$$

where E_L and E_T are the elastic moduli defined in Section 5.1. The time increment Δt is chosen so that the maximum difference in the creep strain increment calculated from the creep strain rate based on the conditions at the beginning and at the end of the increment is always less than CETOL, i.e.,

$$|g_{ij}(\boldsymbol{\sigma}_{n+1} - \boldsymbol{\alpha}_{n+1}) - g_{ij}(\boldsymbol{\sigma}_n - \boldsymbol{\alpha}_n)|\,\Delta t < \text{CETOL} \quad \text{for all } i,j. \tag{62}$$

6.2. *Linearization moduli*

In an implicit finite element code, the overall discretized equilibrium equations are written at the end of the increment, resulting in a set of nonlinear equations for the nodal unknowns. If a full Newton scheme is used to solve the global nonlinear equations, one needs to calculate the so-called 'linearization moduli' $\mathscr{J}$

$$\mathscr{J} = \frac{\partial \boldsymbol{\sigma}_{n+1}}{\partial \boldsymbol{\varepsilon}_{n+1}}. \tag{63}$$

For simplicity, we drop the subscript $(n+1)$ with the understanding that all quantities are evaluated at the end of the increment, unless otherwise indicated. Starting with the elasticity eqn (55), we find

$$\partial\boldsymbol{\sigma} = \mathbf{C}^e : \partial\boldsymbol{\varepsilon} - \mathbf{C}^e : \partial\boldsymbol{\varepsilon}^{cr}, \tag{64}$$

where we took into account that $\partial\,\Delta\boldsymbol{\varepsilon}^{cr} = \partial(\boldsymbol{\varepsilon}^{cr} - \boldsymbol{\varepsilon}_n^{cr}) = \partial\boldsymbol{\varepsilon}^{cr}$.

The differential $\partial\boldsymbol{\varepsilon}^{cr}$ is evaluated from eqns (56) and (57) as follows

$$\partial\boldsymbol{\varepsilon}^{cr} = \Delta t \frac{\partial \mathbf{g}}{\partial \mathbf{s}} : (\partial\boldsymbol{\sigma} - \partial\boldsymbol{\alpha}) \quad \text{where } \mathbf{s} = \boldsymbol{\sigma} - \boldsymbol{\alpha}, \tag{65}$$

$$\partial\boldsymbol{\alpha} = \Delta t \frac{\partial \mathbf{h}}{\partial \mathbf{s}} : (\partial\boldsymbol{\sigma} - \partial\boldsymbol{\alpha}) + \frac{\partial \mathbf{h}}{\partial \dot{\boldsymbol{\sigma}}} : \partial\boldsymbol{\sigma}. \tag{66}$$

Eliminating $\partial\boldsymbol{\alpha}$ from the last two equations, we find

$$\partial\boldsymbol{\varepsilon}^{cr} = \mathbf{D} : \partial\boldsymbol{\sigma}, \tag{67}$$

where

$$\mathbf{D} = \Delta t \frac{\partial \mathbf{g}}{\partial \mathbf{s}} : \left[\mathbf{J} - \left(\mathbf{J} + \Delta t \frac{\partial \mathbf{h}}{\partial \mathbf{s}} \right)^{-1} : \left(\Delta t \frac{\partial \mathbf{h}}{\partial \mathbf{s}} + \frac{\partial \mathbf{h}}{\partial \dot{\boldsymbol{\sigma}}} \right) \right], \tag{68}$$

$\mathbf{J}$ being the fourth-order identity tensor. Finally, substituting eqn (67) into (64) and solving for $\partial\boldsymbol{\sigma}/\partial\boldsymbol{\varepsilon}$, we find

$$\mathscr{J} = \frac{\partial \boldsymbol{\sigma}}{\partial \boldsymbol{\varepsilon}} = (\mathbf{J} + \mathbf{C}^e : \mathbf{D})^{-1} : \mathbf{C}^e = (\mathbf{C}^{e\,-1} + \mathbf{D})^{-1}. \tag{69}$$

6.3. *The case of plane stress*

In this section, we consider the case in which the fibers are all parallel to the $x_3 = 0$ plane (i.e., $\mathbf{n} = n_1\mathbf{e}_1 + n_2\mathbf{e}_2$) and the applied loads are such that $\sigma_{33} = \sigma_{31} = \sigma_{32} = 0$. The stress and strain tensors are now of the form

$$\boldsymbol{\sigma} = \sigma_{\alpha\beta}\mathbf{e}_\alpha\mathbf{e}_\beta \quad \text{and} \quad \boldsymbol{\varepsilon} = \varepsilon_{\alpha\beta}\mathbf{e}_\alpha\mathbf{e}_\beta + \varepsilon_{33}\mathbf{e}_3\mathbf{e}_3, \tag{70}$$

where Greek subscripts range over the integers (1, 2).

In such problems, one has to integrate the constitutive equations for given values of the in-plane components $\Delta\varepsilon_{11}$, $\Delta\varepsilon_{22}$, and $\Delta\varepsilon_{12}$; the out-of-plane component $\Delta\varepsilon_{33}$ is not defined kinematically, and its value is determined so that the condition $\sigma_{33} = 0$ is met. Therefore, some modifications to the method described in Section 6.1 are needed.

The total-strain increment is written as

$$\Delta\boldsymbol{\varepsilon} = \Delta\hat{\boldsymbol{\varepsilon}} + \Delta\varepsilon_{33}\mathbf{e}_3\mathbf{e}_3, \tag{71}$$

where $\Delta\hat{\boldsymbol{\varepsilon}} = \Delta\varepsilon_{\alpha\beta}\mathbf{e}_\alpha\mathbf{e}_\beta$ is the known part of $\Delta\boldsymbol{\varepsilon}$. The plane stress condition $\sigma_{33} = 0$ requires that

$$C^e_{33ij}(\Delta\varepsilon_{ij}-\Delta\varepsilon^{cr}_{ij})=0 \quad \text{or } \Delta\varepsilon_{33}=(C^e_{33ij}\Delta\varepsilon^{cr}_{ij}-C^e_{33\alpha\beta}\Delta\varepsilon_{\alpha\beta})/C^e_{3333}. \tag{72}$$

Using the above expression for $\Delta\varepsilon_{33}$ in the elasticity eqn (55), we find

$$\boldsymbol{\sigma}_{n+1}=\hat{\boldsymbol{\sigma}}^e-\hat{\mathbf{C}}^e:\Delta\boldsymbol{\varepsilon}^{cr}, \tag{73}$$

where

$$\hat{C}^e_{ijkl}=C^e_{ijkl}-C^e_{ij33}C^e_{33kl}/C^e_{3333}, \quad \text{and} \quad \hat{\boldsymbol{\sigma}}^e=\boldsymbol{\sigma}_n+\hat{\mathbf{C}}^e:\Delta\hat{\boldsymbol{\varepsilon}}=\text{known}. \tag{74}$$

In deriving eqn (73), we took into account that $\hat{C}^e_{ijkl}\Delta\varepsilon^{cr}_{kl}=\hat{C}^e_{ij\alpha\beta}\Delta\varepsilon^{cr}_{\alpha\beta}$, since $\Delta\varepsilon^{cr}_{3\alpha}=0$ and $\hat{C}_{ij33}=0$.

The integration procedure becomes now identical to that described in Section 6.1, with $\mathbf{C}^e$ and $\boldsymbol{\sigma}^e$ replaced by $\hat{\mathbf{C}}^e$ and $\hat{\boldsymbol{\sigma}}^e$.

7. AN EXAMPLE: A PLATE WITH A HOLE

The model developed in Section 5 is implemented in the ABAQUS general-purpose finite element program (Hibbitt, 1984). This code provides a general interface so that a specific constitutive model can be introduced as a 'user subroutine'. The constitutive equations are integrated by using the method presented in Section 6.

Figure 9 shows a schematic representation of a plate with a hole. The plate is reinforced by continuous aligned fibers in the x_2 direction. Let $2w$ and l be the width and length of the specimen, and $2a$ be the diameter of the hole; the geometry analyzed is such that $2w/l=6/25$ and $a/w=1/6$.

The matrix material is assumed to be a Ti-6Al-4V alloy and is reinforced by continuous aligned SiC fibers. The fiber volume fraction is 32%, i.e., $f=0.32$. Typical values of the elastic constants for the matrix and the fibers are $E_m=65$ GPa and $\nu_m=0.30$ to Ti-6Al-4V at 600°C, and $E_f=360$ GPa and $\nu_f=0.19$ for SiC at 600°C. The values of the corresponding

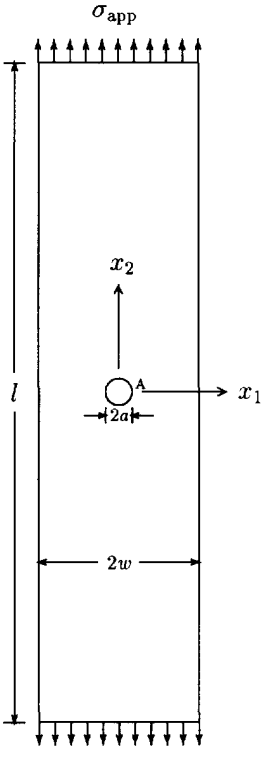

Fig. 9. A plate with a hole. The fibers are in the x_2 coordinate direction.

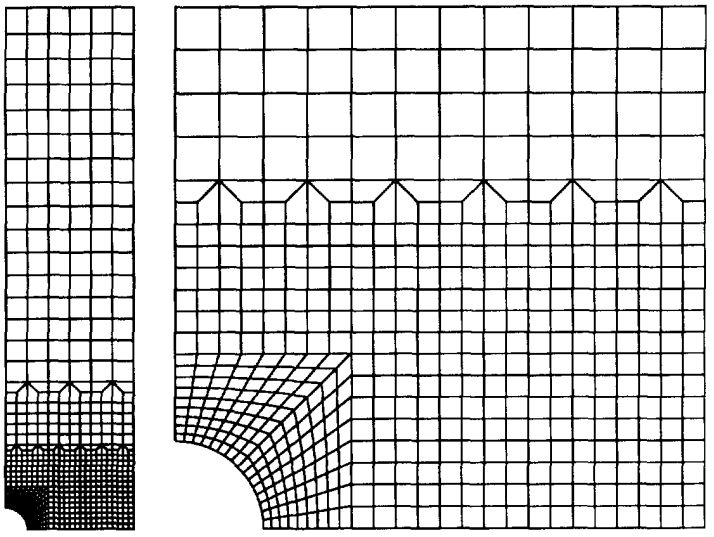

Fig. 10. Finite element mesh for the plate and detailed mesh near the hole.

five effective elastic constants of the composite are calculated from the formulae provided in Section 5.1; the following values are found: $E_L = 160$ GPa, $\nu_T = 0.373$, $\nu_L = 0.259$, $G_T = 34.5$ GPa, and $G_L = 40$ GPa. The effective elastic constants of the composite are also determined from the solution of a series of unit cell problem with periodic boundary conditions; the values found are in very good agreement with those calculated from the formulae of Section 5.1. The creep constants of the matrix are $n = 3$ and $B = 4.125 \times 10^{-13}$ $\text{MPa}^{-n}\,\text{s}^{-1}$.

A tensile stress $\sigma_{app} = 250$ MPa is applied in the direction of the fibers. The thickness of the specimen is assumed to be small, so that plane stress conditions prevail. The load is applied at time $t = 0$, and is kept constant. The instantaneous response of the material is elastic and the elastic stress distribution provides the initial condition for the creep problem.

Due to the symmetries of the structure and the applied loads only one fourth of the plate is analyzed. The finite element mesh used in the calculations is shown in Fig. 10. Four-node isoparametric elements with 2×2 Gauss integrations are used. The analysis is carried out incrementally and the maximum size of the time increment is controlled by the formula in eqn (62).

Figure 11 shows the variations of the axial stress σ_{22} and axial strain ε_{22} ahead of the hole along the cross-fiber direction at time $t = 0^+$, 1, 5, and 8 hours. The maximum values of axial stress and strain appear at the root of the hole (point A in Fig. 9). The same problem is analyzed in Part II, where the possibility fiber failure is examined; it is found that the composite looses its load carrying capacity first in the neighborhood of point A, and eventually fails along the minimum cross-section, as expected. Figure 12 shows contours of the axial stress σ_{22} at time $t = 0^+$, and 8 hours. Contours of the several transversely isotropic invariants of the total strain $\boldsymbol{\varepsilon}$ at time $t = 0^+$ and 8 hours, are shown in Figs 13–16; the invariants plotted in these figures are (deBotton and Ponte Castañeda, 1993):

$$\varepsilon_p = \tfrac{1}{2}\boldsymbol{\varepsilon} : \boldsymbol{\beta} = \tfrac{1}{2}(\varepsilon_{11} + \varepsilon_{33}), \tag{75}$$

$$\varepsilon_n = \boldsymbol{\varepsilon} : \mathbf{a} = \varepsilon_{22}, \tag{76}$$

$$\gamma_p^2 = \tfrac{1}{2}(\boldsymbol{\varepsilon} \cdot \boldsymbol{\beta}) : (\boldsymbol{\varepsilon} \cdot \boldsymbol{\beta}) - \tfrac{1}{4}(\boldsymbol{\varepsilon} : \boldsymbol{\beta})^2 = \varepsilon_{13}^2 + \tfrac{1}{4}(\varepsilon_{11} - \varepsilon_{33})^2, \tag{77}$$

$$\gamma_n^2 = \boldsymbol{\varepsilon}^2 : \mathbf{a} - (\boldsymbol{\varepsilon} : \mathbf{a})^2 = \varepsilon_{12}^2 + \varepsilon_{23}^2, \tag{78}$$

where $\mathbf{n} = \mathbf{e}_2$, $\boldsymbol{\beta} = \mathbf{I} - \mathbf{nn} = \mathbf{e}_1\mathbf{e}_1 + \mathbf{e}_3\mathbf{e}_3$, and the Cartesian components refer to the coordinate system shown in Fig. 9. The axial strain ε_n and the transverse 'dilatational' strain ε_p attain

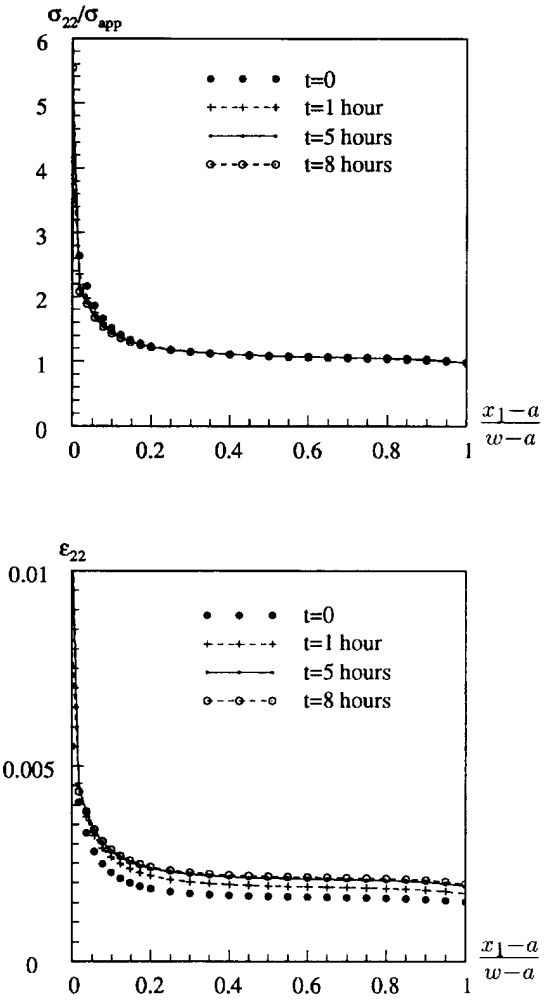

Fig. 11. Variations of the normalized axial stress σ_{22}/σ_{app}, and the axial strain ε_{22} along the cross-fiber direction at time $t = 0^+$, 1, 5 and 8 hours.

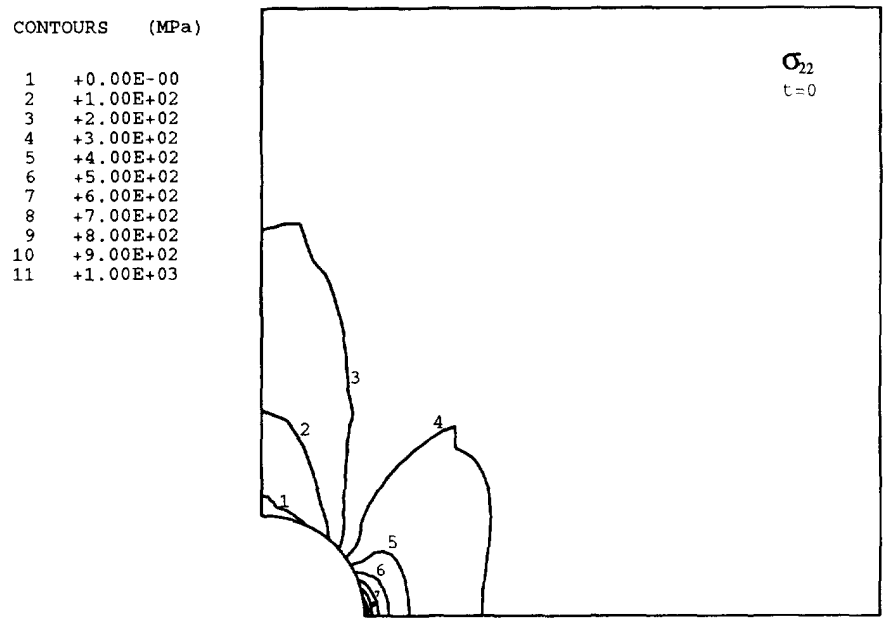

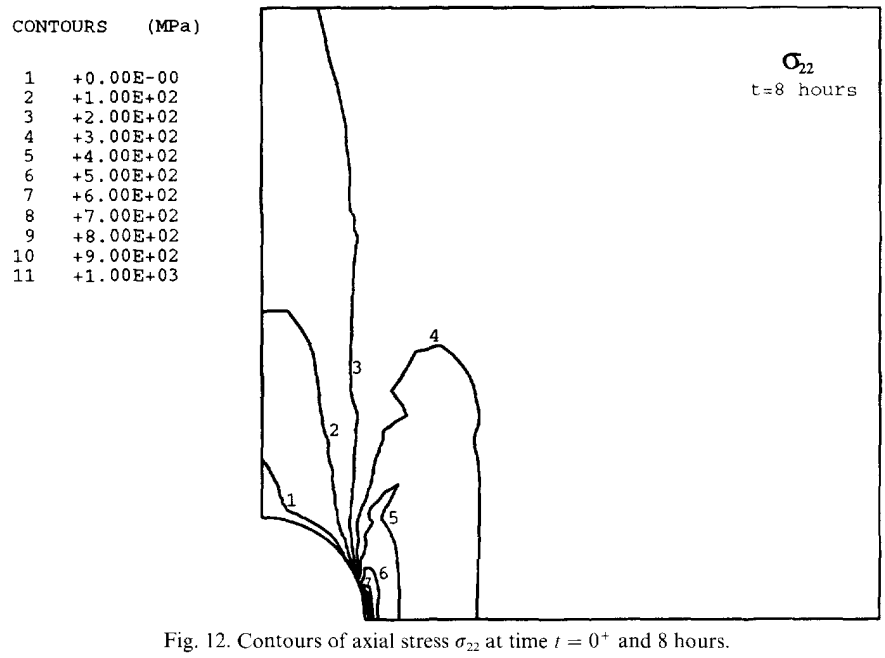

Fig. 12. Contours of axial stress σ_{22} at time $t = 0^+$ and 8 hours.

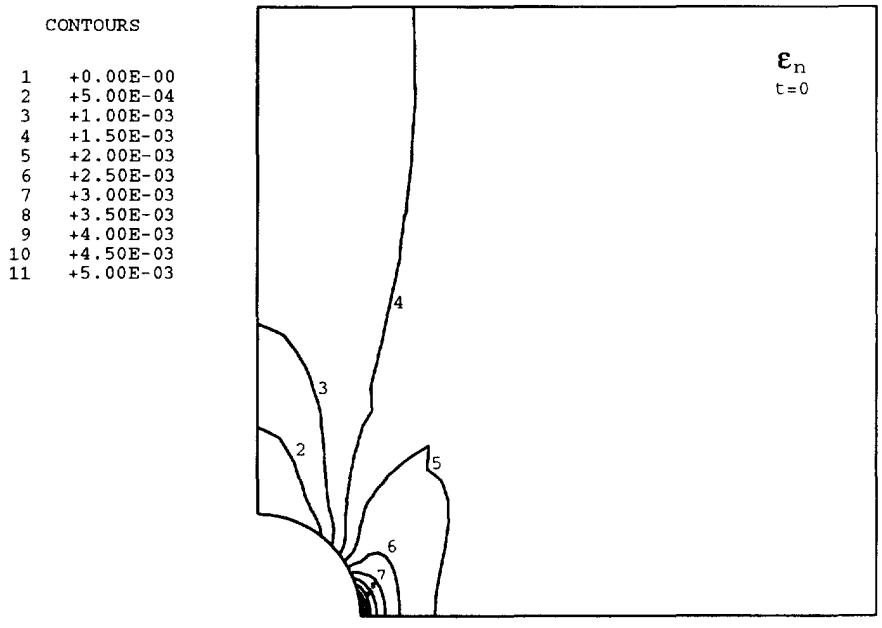

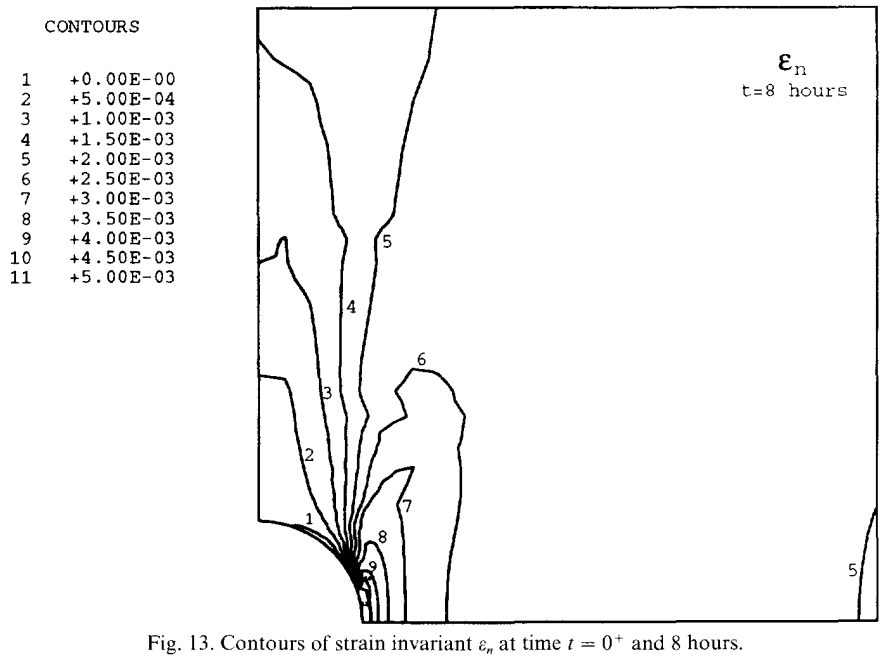

Fig. 13. Contours of strain invariant ε_n at time $t = 0^+$ and 8 hours.

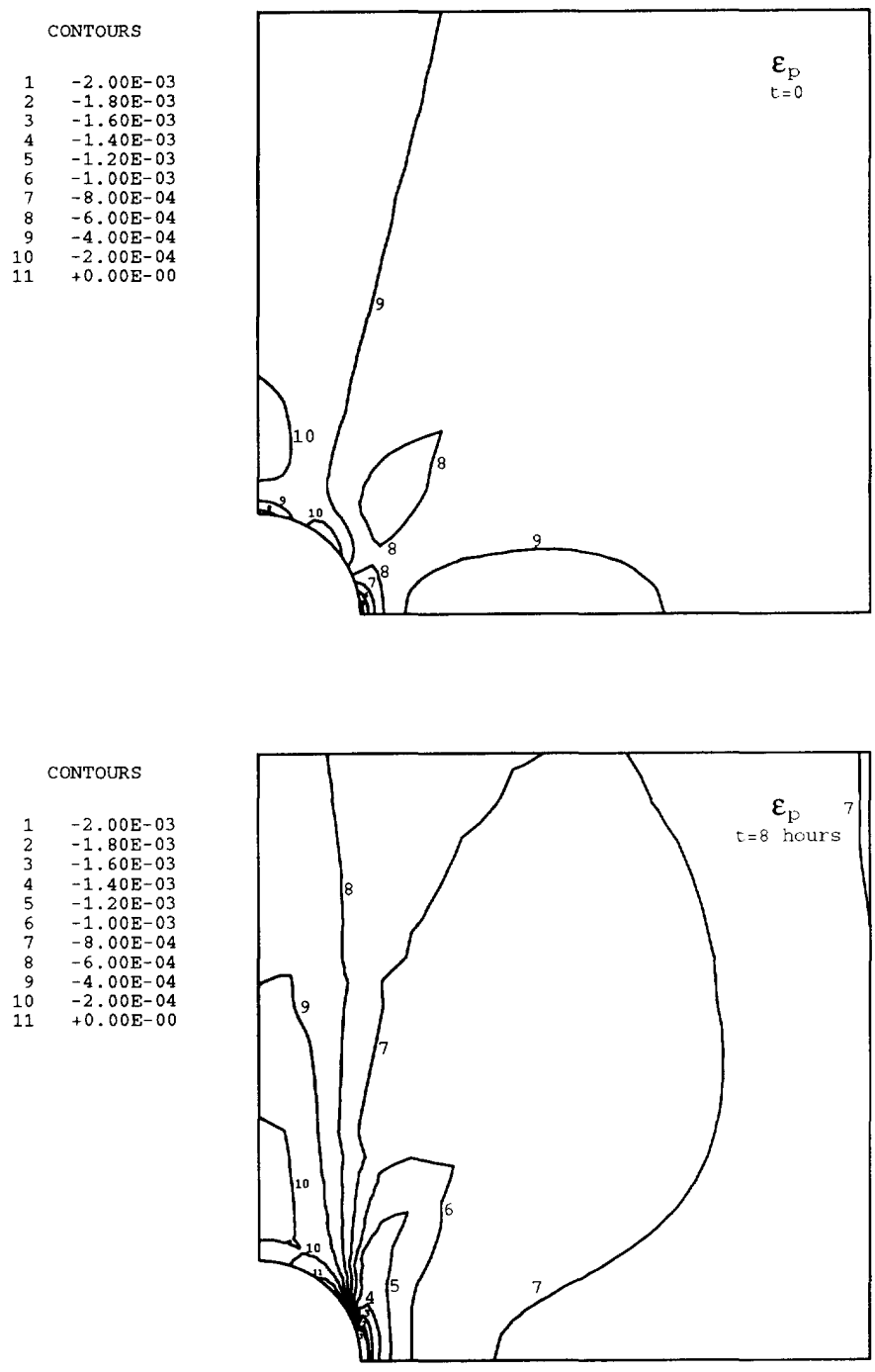

Fig. 14. Contours of strain invariant ε_p at time $t = 0^+$ and 8 hours.

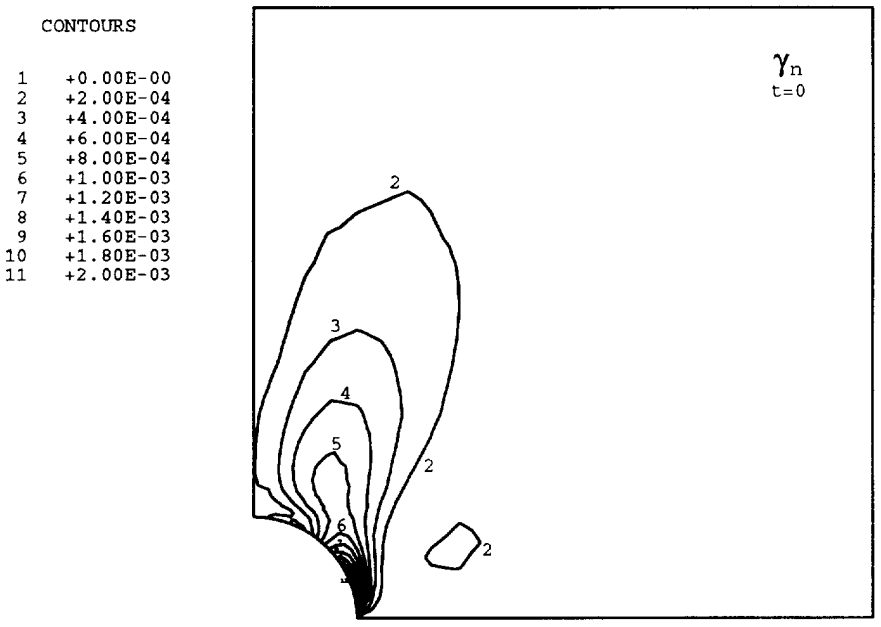

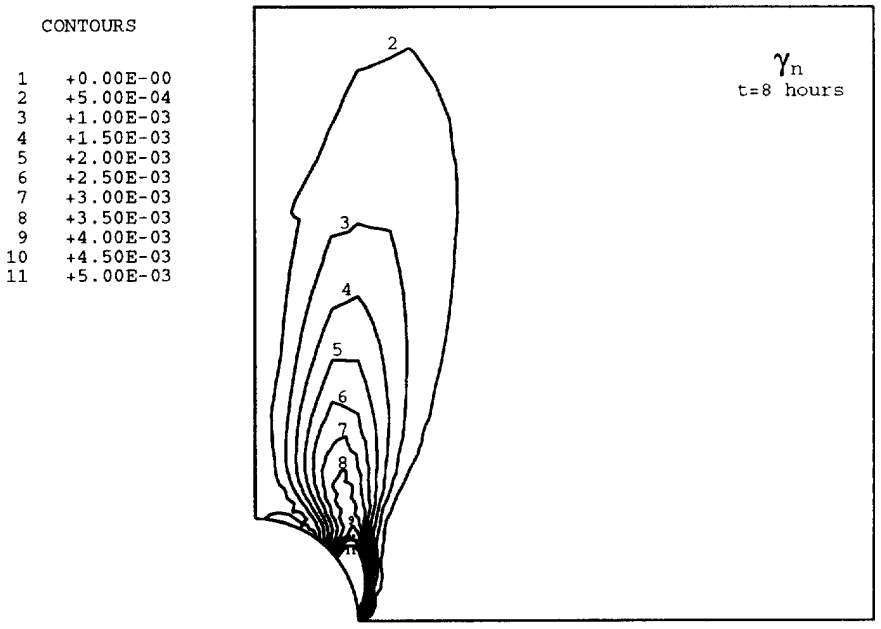

Fig. 15. Contours of strain invariant γ_n at time $t = 0^+$ and 8 hours.

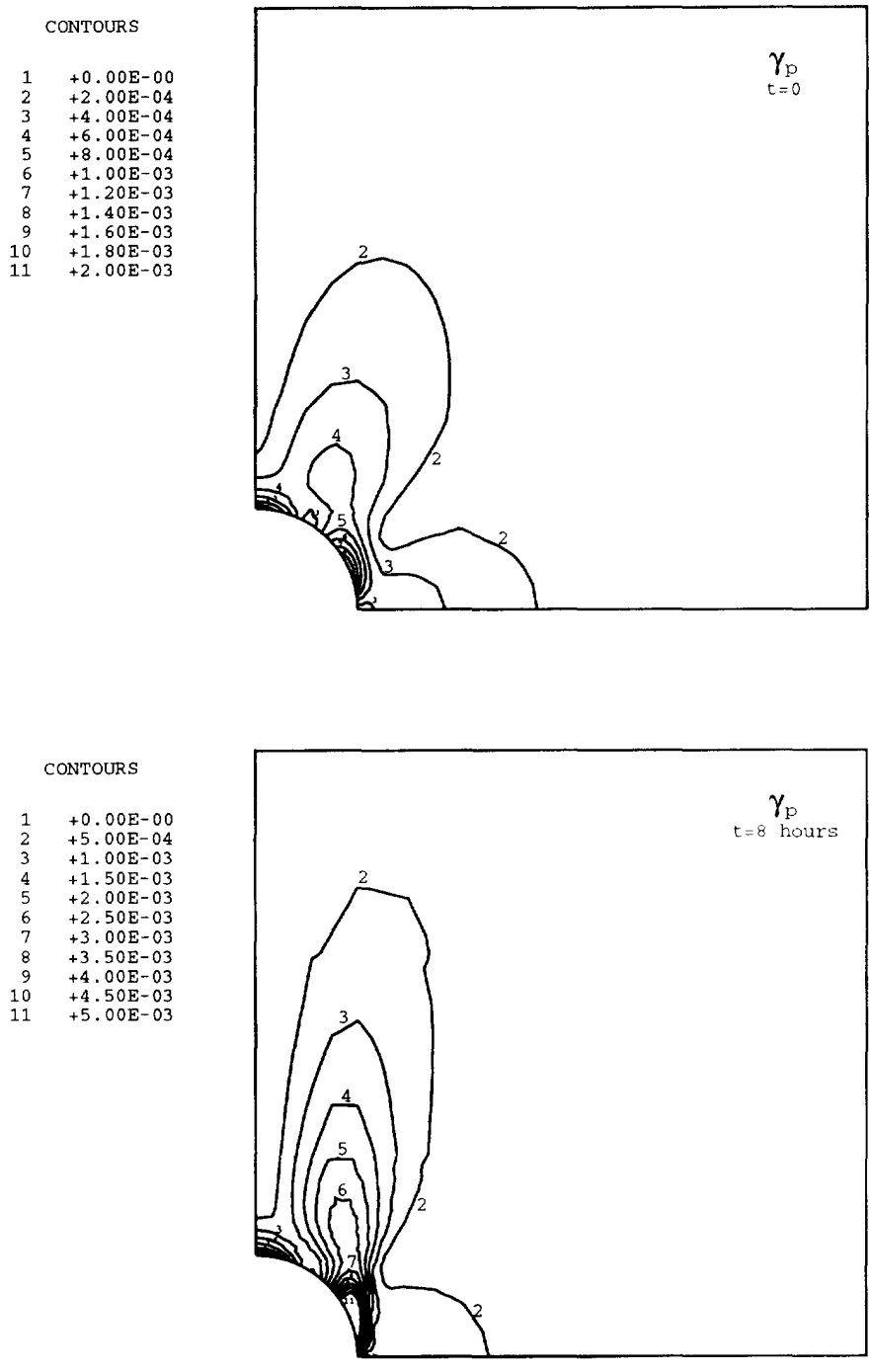

Fig. 16. Contours of strain invariant γ_p at time $t = 0^+$ and 8 hours.

their maximum values at point A. Figures 15 and 16 show that the longitudinal (γ_n) and transverse (γ_p) shear strains reach their maximum values on the surface of the hole; fiber debonding is to be expected in those locations.

Acknowledgements—Fruitful discussions with Professor R. M. McMeeking of the University of California, Santa Barbara are gratefully acknowledged. This research was supported by the Office of Naval Research contract N00014-92-J-1808 through sub-agreement KK3006 from the University of California, Santa Barbara. The ABAQUS finite element code was made available under academic license from Hibbitt, Karlsson and Sorensen, Inc., Providence, RI.

REFERENCES

Aravas, N., Cheng, C. and Ponte Castañeda, P. (1995) Steady state creep of fiber-reinforced composites: constitutive equations and computational issues. *International Journal of Solids and Structures* **32,** 2219–2244.

Bakhvalov, N. and Panasenko, G. (1989) *Homogenization: Averaging Processes in Periodic Media.* Kluwer Academic Publishers, Dordrecht, The Netherlands.

Cheng, C. (1996) Creep of fiber-reinforced metal-matrix composites. Ph.D. thesis, Department of Mechanical Engineering and Applied Mechanics, University of Pennsylvania.

Christensen, R. M. (1979) *Mechanics of Composite Materials.* Wiley, New York.

deBotton, G, and Ponte Castañeda, P. (1993) Elastoplastic constitutive relations for fiber-reinforced solids. *International Journal of Solids and Structures* **30,** 1865–1890.

Goto, S. and McLean, M. (1991a) Role of interfaces in creep of fibre-reinforced metal-matrix composites—I. Continuous fibers. *Acta Metallica Materiala* **39,** 153–164.

Goto, S. and McLean, M. (1991b) Role of interfaces in creep of fibre-reinforced metal-matrix composites—II. Short fibers. *Acta Metalica Materiala* **39,** 165–177.

Hibbitt, H. D. (1984) ABAQUS/EPGEN—A general purpose finite element code with emphasis on nonlinear applications. *Nuclear Engineering Design* **7,** 271–297.

Johnson, A. F. (1977) Creep characterization of transversely-isotropic metallic materials. *Journal of the Mechanics and Physics of Solids* **25,** 117–126.

Kelly, A. and Street, N. Creep of discontinuous fibre composites II. Theory for the steady state. *Proceedings of the Royal Society, London* **328,** 283–293.

McLean, M. (1985) Creep deformation of metal-matrix composites. *Composites Science Technology* **23,** 37–52.

McLean, M. (1988) Mechanics and models of high temperature deformation of composites. *Materials Research Symposium Proceedings* **120,** 67–79.

McLean, M. (1989) Creep of metal matrix composites. In *Materials and Engineering Design: The Next Decade,* eds B. F. Dyson and D. R. Hayhurst, p. 287. Institute of Metals, London.

McMeeking, R. M. (1993a) Models for the creep of ceramic matrix composite materials. In *High Temperature Mechanical Behavior of Ceramic Composites,* eds S. V. Nair and K. Jakus, p. 409. Butterworth-Heinemann, Stoneham, Mass.

McMeeking, R. M. (1993b) Power law creep of a composite material containing discontinuous rigid aligned fibers. *International Journal of Solids and Structures* **30,** 1807–1823.

Mileiko, S. T. (1970) Steady state creep of a composite material with short fibres. *Journal of Material Science* **5,** 254–261.

Ponte Castañeda, P. (1996) Exact second-order estimates for the effective mechanical properties of nonlinear composite materials. *Journal of the Mechanics and Physics of Solids* **44,** 827–862.

Sanchez Palencia, E. (1980) *Non-homogeneous Media and Vibration Theory.* Lecture Notes in Physics, Vol. 127. Springer-Verlag, Berlin.

Weber, C. H., Löfvander, J. P. A. and Evans, A. G. (1993) The creep behavior of CAS/Nicalon continuous-fiber composites. *Acta Metallica Materiala* **41,** 2681–2690.